

Shape transformation of vesicles induced by orientational arrangement of membrane proteins

Menglong Feng(冯梦龙), Kunhao Dong(董堃昊), Yuansheng Cao(曹远胜), and Rui Ma(马锐)
Citation: Chin. Phys. B, 2025, 34 (**8**): 088706. DOI: 10.1088/1674-1056/adc36d
http://cpb.iphy.ac.cn; http://iopscience.iop.org/cpb

What follows is a list of articles you may be interested in

Effects of electric field on vibrational resonances in Hindmarsh-Rose neuronal systems for signal detection

Xiaoxia Li(李晓霞), Xiaopeng Xue(薛小鹏), Dongjie Liu(刘栋杰), Tianyi Yu(余天意), Qianqian He(何倩倩), and Guizhi Xu(徐桂芝)
Chin. Phys. B, 2023, 32 (**4**): 048701. DOI: 10.1088/1674-1056/ac9cc0

Transmembrane transport of multicomponent liposome-nanoparticles into giant vesicles

Hui-Fang Wang(王慧芳), Chun-Rong Li(李春蓉), Min-Na Sun(孙敏娜), Jun-Xing Pan(潘俊星), and Jin-Jun Zhang(张进军)
Chin. Phys. B, 2022, 31 (**4**): 048703. DOI: 10.1088/1674-1056/ac380f

Estimation of biophysical properties of cell exposed to electric field

Hui Zhang(张辉), Liyang Wang(王李阳), Peijie Zhang(张培杰), Xiaodi Zhang(张小娣), and Jun Ma(马军)
Chin. Phys. B, 2021, 30 (**3**): 038702. DOI: 10.1088/1674-1056/abc543

Dielectric properties of nucleated erythrocytes as simulated by the double spherical-shell model

Jia Xu(徐佳), Weizhen Xie(谢伟珍), Yiyong Chen(陈一勇), Lihong Wang(王立洪), and Qing Ma(马青)
Chin. Phys. B, 2020, 29 (**12**): 128703. DOI: 10.1088/1674-1056/abbbf0

Tail-structure regulated phase behaviors of a lipid bilayer

Wenwen Li(李文文), Zhao Lin(林召), Bing Yuan(元冰), and Kai Yang(杨恺)\ccclink
Chin. Phys. B, 2020, 29 (**12**): 128701. DOI: 10.1088/1674-1056/abad20

SPECIAL TOPIC — A celebration of the 90th Anniversary of the Birth of Bolin Hao

Shape transformation of vesicles induced by orientational arrangement of membrane proteins

Menglong Feng(冯梦龙)[1,†], Kunhao Dong(董堃昊)[1,†], Yuansheng Cao(曹远胜)[2,‡], and Rui Ma(马锐)[3,§]

[1] *Department of Physics, College of Physical Science and Technology, Xiamen University, Xiamen* 361005, *China*
[2] *Department of Physics, Tsinghua University, Beijing* 100084, *China*
[3] *Fujian Provincial Key Laboratory for Soft Functional Materials Research, Research Institute for Biomimetics and Soft Matter, Department of Physics, College of Physical Science and Technology, Xiamen University, Xiamen* 361005, *China*

(Received 1 March 2025; revised manuscript received 12 March 2025; accepted manuscript online 21 March 2025)

Vesicles of lipid bilayer can adopt a variety of shapes due to different coating proteins. The ability of proteins to reshape membrane is typically characterized by inducing spontaneous curvature of the membrane at the coated area. BAR family proteins are known to have a crescent shape and can induce membrane curvature along their concaved body axis but not in the perpendicular direction. We model this type of proteins as a rod-shaped molecule with an orientation and induce normal curvature along its orientation in the tangential plane of the membrane surface. We show how a ring of these proteins reshapes an axisymmetric vesicle when the protein curvature or orientation is varied. A discontinuous shape transformation from a protrusion shape without a neck to a one with a neck is found. Increasing the rigidity of the protein ring is able to smooth out the transition. Furthermore, we show that varying the protein orientation is able to induce an hourglass-shaped neck, which is significantly narrower than the reciprocal of the protein curvature. Our results offer a new angle to rationalize the helical structure formed by many proteins that carry out membrane fission functions.

Keywords: cell membrane, BAR proteins, anisotropic curvature, shape transformation

PACS: 87.15.kt, 87.15.K–, 87.17.Rt, 87.10.–e

DOI: 10.1088/1674-1056/adc36d **CSTR:** 32038.14.CPB.adc36d

1. Introduction

Cells are able to remodel their shapes to perform specific biological functions. A small vesicle buds off from the plasma membrane during endocytosis.[1,2] A mother cell is divided into two daughter cells during mitosis.[3,4] A crawling cell forms protrusions at the leading edge when migrating on a substrate.[5] The various morphology of cells is attributed to proteins that either induce membrane curvatures or produce forces to deform the membrane.[6] Besides the entire shape, membrane curvature can also cause the lipid segregation[7] Clathrin molecules can assemble into a cage-like structure and scaffold the membrane into a spherical vesicle.[8] BAR family proteins, initially identified in yeast cells,[9,10] regulate the shape of membranes in various biological processes, including endocytosis,[11] autophagy,[12] cell division,[13] motor transportation[14] and membrane remodelling.[15] Meanwhile, their interaction with other cellular structures such as plasma membrane,[16] cytoskeletons,[17] and dynamin[18,19] can play an important role.[20,21] Due to the crescent shape of the BAR proteins, they tend to curve the membrane along the direction of their body axis, thus remodelling the membrane into a tubular shape.[22] Even though different BAR proteins vary in their length, intrinsic curvature, and binding affinity to the membrane, the ability to induce membrane tubulation is a common property for most of the BAR proteins.[23] The classical BAR and N-BAR proteins containing a unique N-terminal amphipathic helix[24] can generate tubules, with diameters from 20 nm to 60 nm,[25] and bend the membrane towards the leaflet in which they are embedded. On the microscale, N-terminal amphiphilic helices can bend the membrane by adjusting the insertion depth.[26] F-BAR proteins can induce wider tubules from 60 nm to 100 nm[27,28] in diameter and also bend the membrane towards the attached leaflet. By contrast, I-BAR proteins induce curvatures towards the unattached leaflet.[29,30] When bound to the inner leaflet of a closed vesicle, I-BAR proteins are able to produce membrane protrusions.[31] The ability of BAR proteins to remodel the membrane depends on the protein density,[32] as well as the mechanical properties of the membrane,[33] such as membrane tension and bending rigidity.[34,35] BAR proteins can scaffold membranes into tubular shapes at high density. However, at low density, they bind to sites with preferred curvatures on the membrane, acting as a curvature sensor.[36]

The organization of BAR proteins also plays an important role when generating membrane curvatures.[37–39] Both biological experiments and molecular dynamics simulations

[†]These authors contributed equally to this work.
[‡]Corresponding author. E-mail: yscao@tsinghua.edu.cn
[§]Corresponding author. E-mail: ruima@xmu.edu.cn

© 2025 Chinese Physical Society and IOP Publishing Ltd. All rights, including for text and data mining, AI training, and similar technologies, are reserved.

have been applied to investigate their functions during membrane remodeling.[40] Computer simulations have shown that crescent-shaped molecules can remodel a vesicle into the polygonal shape with the corners formed by aggregates of the molecules.[41] In a coarse-grained molecular dynamics simulation, BAR proteins at low surface densities form string-like aggregates and meshes which induce deep invaginations on the membrane.[42] On a tubular membrane, a study based on a mean field theory of rod-shaped molecules has shown that with increasing surface density, the proteins undergo a phase transition from an isotropic phase to a nematic phase due to the entropic interactions that arise from the excluded volume effect.[43] In the nematic phase, proteins tend to align with each other and form a tilted angle relative to the azimuthal direction of the tubular surface. In a recent study, BAR proteins are shown to be enriched in the neck region of a membrane and induce neck elongation and tube pearling both in theory and experiments.[44]

In this paper, we study the deformation of a spherical vesicle induced by a ring of proteins that produce normal curvature along a tangential direction on the membrane and focus on how the orientation of the proteins influences the shape of the vesicle. The paper is organized as follows. Firstly, we will illustrate the geometry of an axisymmetric surface and formulate our theoretical model of lipid membrane coated by anisotropic proteins. Secondly, we will show the membrane shapes acquired by our numerical method, where shape diagrams with respect to the preferred curvature and protein orientation are displayed to reveal the shape transformation. Thirdly, we will elaborate how other factors including coating position and the bending rigidity influence the cellular morphology and shape transformation. Finally, we will summarize this work and compare our results with similar research on anisotropic proteins.

2. Mechanical model of membrane and proteins

2.1. Geometric representation of the membrane surface

We consider an axisymmetric membrane vesicle whose shape is parameterized as (Fig. 1).

$$\boldsymbol{X}(u,\phi) = [r(u)\cos\phi, r(u)\sin\phi, z(u)], \tag{1}$$

where $\phi \in [0, 2\pi]$ is the azimuthal coordinate, $u \in [0,1]$ is a dimensionless coordinate to label the meridional position with $u = 0$ and $u = 1$ indicating the north pole and the south pole respectively. We introduce two auxiliary functions $\psi(u)$ and $h(u)$, which fulfill the geometric relations

$$\frac{\mathrm{d}r}{\mathrm{d}u} = h\cos\psi, \tag{2}$$

$$\frac{\mathrm{d}z}{\mathrm{d}u} = -h\sin\psi. \tag{3}$$

The function $\psi(u)$ represents the angle spanned between the tangential direction along the meridian and the radial direction. As for the function $h(u)$, we require $\mathrm{d}h/\mathrm{d}u = 0$ which means $h(u)$ is a constant. Because of the relation $h = \sqrt{(\mathrm{d}r/\mathrm{d}u)^2 + (\mathrm{d}r/\mathrm{d}z)^2} = \mathrm{d}s/\mathrm{d}u$, where $s(u)$ denotes the arc length calculated from the north pole, h is equal to the total arc length S from the north pole to the south pole. With the help of the two auxiliary functions $\psi(u)$ and $h(u)$, the two principal curvatures of the membrane surface can be simplified as

$$C_1 = \frac{1}{h}\frac{\mathrm{d}\psi}{\mathrm{d}u}, \tag{4}$$

$$C_2 = \frac{\sin\psi}{r}. \tag{5}$$

We also introduce the auxiliary function $A(u)$ to denote the surface area of the membrane patch ranging from the north pole to the circumferential line with the coordinate u. It satisfies the equation

$$\frac{\mathrm{d}A}{\mathrm{d}u} = 2\pi r h. \tag{6}$$

The total surface area of the vesicle $A_0 = 4\pi R_0^2$ is conserved during deformation, which is imposed by the boundary condition $A(0) = 0$ and $A(1) = A_0$.

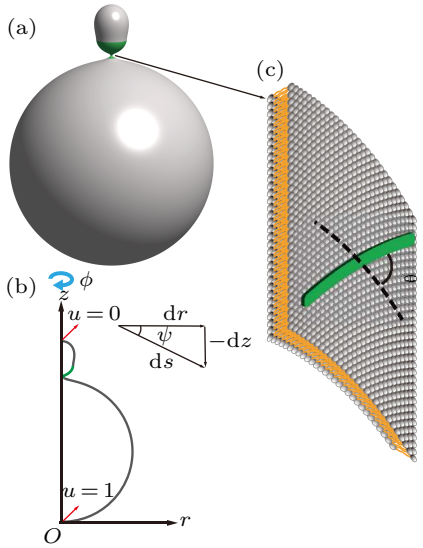


Fig. 1. (a) Schematic illustration of the neck formed by coating proteins that are tilted relative to the azimuthal direction on the membrane. The proteins are assumed to be rod-shaped and tend to bend the membrane along their body orientation. (b) Geometric representation of a closed axisymmetric surface. The green part represents the protein coated region which forms a ring.

2.2. Free energy of the membrane vesicle

We employ the Helfrich theory to model the membrane whose free energy reads[45,46]

$$F_{\mathrm{m}} = \int \frac{\kappa_{\mathrm{m}}}{2}(C_1 + C_2 - C_{\mathrm{m}})^2\,\mathrm{d}A + pV, \tag{7}$$

where κ_{m} denotes the bending rigidity of the membrane, C_{m} denotes the spontaneous curvature. It serves as a successful

model to describe the bending of the membrane and a first integral can be found for an axisymmetric surface.[47,48] In the Helfrich bending energy, we neglect the contribution from the Gaussian curvature term, $\bar{\kappa}_{\rm m}\int C_1C_2\,{\rm d}A$, which is a constant for a vesicle of spherical topology due to the famous Gauss-Bonnet theorem.[49] We set the spontaneous curvature of the membrane $C_{\rm m}$ to zero and focus on the membrane deformation induced by the BAR proteins, which will be described later. The vesicle encloses a volume of V and has a pressure difference $p = p_{\rm out} - p_{\rm in}$ between outside and inside. We fix the pressure difference $p = -15\ \kappa_{\rm m}/R_0^3$ and allow the volume V to change. The negative sign implies that the inner pressure is higher than the outer pressure. The pressure term, however, will become much more significant when it comes to the yeast cells, where vesicles have to overcome huge pressure difference to enter the cell.[50] Considering the typical value for the membrane bending rigidity $\kappa_{\rm m} = 20\,k_{\rm B}T$ and the size of a vesicle of 100 nm in diameter, the pressure difference p is about 0.01 MPa. We also perform calculations in the limit of $p = 0$ and the results only change quantitatively but not qualitatively (data not shown).

We introduce a Lagrangian multiplier γ, which serves as the membrane tension, to impose the geometric relation in Eq. (6). For a homogeneous membrane, the function $\gamma(u)$ is a constant. For an inhomogeneous membrane due to protein coat, $\gamma(u)$ becomes a spatially varied function that fulfills Eq. (B6) in Appendix B.

2.3. Free energy of the protein coat

The rod-shaped BAR proteins are assumed to be recruited on the axisymmetric membrane surface and form a ring along the azimuthal direction. The ring only covers a tiny fraction (1%) of the membrane area and is located at $A_1 < A(u) < A_2$. The coating area of proteins $A_{\rm coat} = A_2 - A_1$, and the coating position is indicated by the average $(A_1 + A_2)/2$. Within the ring, the density of the proteins is high enough to ensure that they are in the nematic phase and oriented in the same direction,[43] forming a tilted angle θ with the azimuthal direction (Fig. 1(c)). From Euler's formula,[49] the normal curvature along the θ direction reads

$$C_\theta = \frac{\sin\psi}{r}\cos^2\theta + \frac{1}{h}\frac{{\rm d}\psi}{{\rm d}u}\sin^2\theta. \tag{8}$$

Deviation of the normal curvature C_θ of the membrane surface from the proteins' preferred curvature $C_{\rm p}$ leads to the anisotropic bending energy of the BAR proteins[37,44,51,52]

$$F_{\rm p} = \int \frac{\kappa_{\rm c}}{2}\left(C_\theta - C_{\rm p}\right)^2 {\rm d}A, \tag{9}$$

where $\kappa_{\rm c}$ denotes the bending rigidity of the protein coat. Since the ring of proteins is bound to the membrane only at $A_1 < A(u) < A_2$, $\kappa_{\rm c}$ is taken as a function of $A(u)$

$$\kappa_{\rm c}[A(u)] = \begin{cases} \kappa_{\rm p}, & \text{if}\ \ A_1 < A(u) < A_2, \\ 0, & \text{otherwise.} \end{cases} \tag{10}$$

In practice, we approximate the piecewise function as

$$\kappa_{\rm c}[A(u)] = \frac{\kappa_{\rm p}}{2}\{\tanh[S_{\rm p}(A(u) - A_1)] - \tanh[S_{\rm p}(A(u) - A_2)]\}, \tag{11}$$

where $S_{\rm p}$ is a parameter to control the sharpness of the protein edge.

2.4. Variational equations

Summing up the contributions from both the membrane $F_{\rm m}$ and the protein coat $F_{\rm p}$, as well as the Lagrangian multipliers $F_{\rm L}$ to enforce the geometric relations (2), (3) and (6) (see Appendix A for the explicit expression of $F_{\rm L}$), we express the effective total free energy $F_{\rm tot}$ of the system as a functional of the geometric variables r, z, ψ, h, $\bar{A}$, and the Lagrangian multipliers α, β, γ:

$$F_{\rm tot} = F_{\rm m} + F_{\rm p} + F_{\rm L} = 2\pi\int_0^1 \mathcal{F}[r, z, \psi, h, \bar{A}, \alpha, \beta, \gamma]\,{\rm d}u. \tag{12}$$

Here $\bar{A}(u) = A(u)/(2\pi)$ is the reduced surface area function. We then perform variations with respect to the functions $\{\psi(u), r(u), z(u), \bar{A}(u), \alpha(u), \beta(u), \gamma(u)\}$ to obtain the Euler–Lagrange equations

$$\frac{\delta F_{\rm tot}}{\delta X} = \frac{\partial \mathcal{F}}{\partial X} - \frac{\rm d}{{\rm d}u}\left(\frac{\partial \mathcal{F}}{\partial X'}\right) = 0, \tag{13}$$

where X denotes one of the functions and X' refers to their derivatives with respect to u. The explicit expressions for the Euler–Lagrange equations and the associated boundary conditions are provided in Appendix B.

We numerically solve the Euler–Lagrange equations with the MATLAB solver bvp5c that is designed for boundary value problems. We fix either the protein curvature $C_{\rm p}$ or the tilted angle θ and iteratively vary the other to obtain the corresponding membrane shape and the free energy. Using the free energy curve, we construct the phase diagram of the membrane shape as a function of $C_{\rm p}$ and θ. The details are provided in Appendix B.

3. Results

3.1. Shape transformations by a protein ring near the north pole

We first study the shape transformations of the spherical vesicle when the protein ring is located near the north pole with $(A_1 + A_2)/(2A_0) = 0.033$. Because a soft protein coat cannot dramatically deform the spherical vesicle (data not shown), we set the bending rigidity of the protein ring twice as rigid as the membrane, i.e., $\kappa_{\rm p} = 2\kappa_{\rm m}$, which is already able to induce significant deformation of the vesicle when varying the protein curvature $C_{\rm p}$ or the tilted angle θ. The results for very rigid protein coat will be shown later in Subsection 3.3. When the the tilted angle is relatively high, for instance, $\theta = 46°$,

continuously varying the protein curvature C_p transforms the spherical vesicle into a vase-like shape with the protein coated region growing outward and forming a high positive curvature bump (Fig. 2(a)). This is because the proteins tend to produce positive curvature along the meridional direction. However, with a relatively small tilted angle $\theta = 22°$, two types of shapes emerge as C_p goes up. A protrusion, which is characterized by a region with negative curvature C_1, is formed at relatively small C_p (Fig. 2(b), shapes labeled with A, B, C). Another type of solution features a shape in which the protein ring is contracted inward to form a protrusion with a narrow neck (Fig. 2(b), shapes labeled with D, E, F). The two types of shapes are connected with a Gibbs triangle in the total free energy curve, which indicates a first-order (discontinuous) phase transition at the crossing point (Fig. 2, pink curve, $C_pR_0 = 18.81$). Note that on the branch from shape D to F in Fig. 2(b), the neck induced by the proteins grows narrower and longer with increasing C_p. The shape resembles the tubulation induced by N-BAR proteins observed in experiments.[53] Experiments also confirm a series of similar shapes during the neck formation.[54] This is because proteins are aligned almost in parallel with the azimuthal direction and tend to contract the membrane to a radius that is close to their preferred curvature C_p.

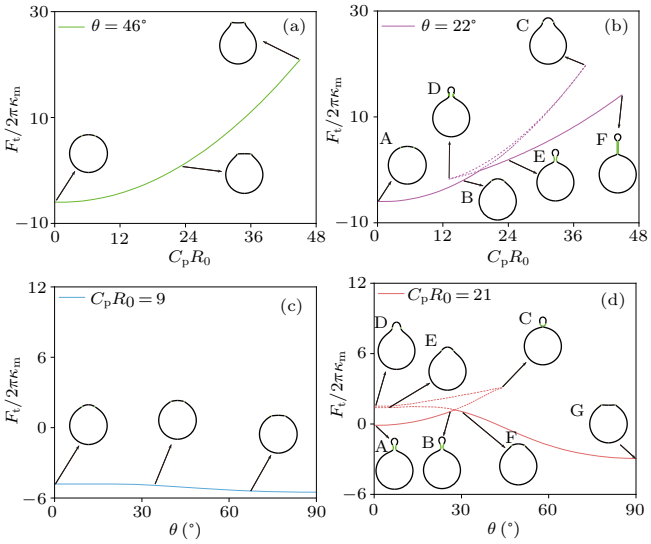


Fig. 2. Free energy curves and the associated shape transformations of a vesicle induced by varying the protein curvature C_p in (a), (b) or the protein orientation θ in (c), (d). The solid lines indicate the minimum free energy state and the dash lines indicate states with higher free energy. The protein ring is located near the north pole where $(A_1+A_2)/(2A_0) = 0.033$, and has bending rigidity $\kappa_p/\kappa_m = 2$.

We now investigate how continuously varying the tilted angle θ transforms the membrane shapes. When the protein curvature C_p is small, e.g., $C_pR_0 = 9$, increasing θ from 0° to 90° only slightly changes the vesicle shape such that the protrusion formed at small θ is flattened or even bent inward at large θ (Fig. 2(c)). If the protein curvature C_p is raised to $C_pR_0 = 21$, at relatively small θ, a single θ corresponds to three solutions of protrusion shapes, two of which have no neck and the third one has a neck. It is intriguing to see that as θ goes up, the neck is narrowed down to a very small radius (Fig. 2(d), see shapes labeled with A, B and C), which could induce a small vesicle budding off the membrane. This necking phenomenon will be further discussed later in the paper. Meanwhile, the branch without necks goes from a protrusion shape to a vase-like shape such that the bulge is flattened (Fig. 2(d), see shapes labeled with E, F and G). The two branches cross at a critical point in a Gibbs triangle, which indicates a first-order phase transition from a protrusion with neck to a protrusion without neck with increasing θ (Fig. 2(d), shapes labeled from B to F).

The anisotropic spontaneous curvature can usually cause tubular shapes of the membrane, as reported in references.[55,56] Early works have shown that the anisotropic protein can help to stabilize the neck.[57,58] To systematically understand the shape transformations induced by the protein curvature C_p and the tilted angle θ, we show the phase diagram in Fig. 3. The phase space is divided into two regions, depending on whether the protrusions have a neck or not. Crossing the boundary from one region to the other represents a first-order phase transition characterized by the Gibbs triangle exemplified in Figs. 2(b) and 2(d). As θ goes from 0° (parallel to the azimuthal direction) to about 45°, an increasing protein curvature C_p is needed for necking to occur. Within the necking region, the radius of the neck is reduced with increasing C_p, while the length of the neck is elongated (Fig. 3, dots in purple). Beyond $\theta = 45°$, necking cannot occur anymore.

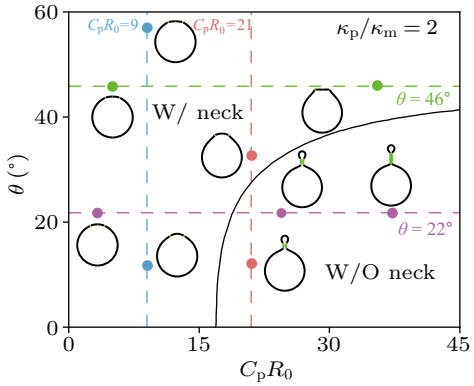


Fig. 3. Phase diagram of vesicle shapes as a function of the protein curvature C_p and the protein orientation θ. The solid line represents the boundary that separates the region of a protrusion shape without a neck from a region with a neck. Crossing the boundary leads to a discontinuous transition of the vesicle morphology. The four colored dashed lines represent the situation studied in Fig. 2. The protein ring is located near the north pole where $(A_1+A_2)/(2A_0) = 0.033$, and has bending rigidity $\kappa_p/\kappa_m = 2$.

3.2. Shape transformations by a protein ring at the equator

We now place the protein ring at the equator, i.e., $(A_1 + A_2)/(2A_0) = 0.5$, and investigate the deformation of the spherical vesicles when varying C_p and θ. If θ takes a value that is larger than 45°, e.g., $\theta = 46°$, varying C_p only slightly alters

the spherical vesicle into a rugby shape (Fig. 4(a)). However, when θ is small, such that the proteins are oriented mainly in parallel with the azimuthal direction, we observe two types of solutions connected by a Gibbs triangle in the free energy curve (Fig. 4(b)).

On one of them (Fig. 4(b), shapes labeled with A, B and C), shape transformations are similar to those of $\theta = 46°$. While on the other (Fig. 4(b), shapes labeled with D, E and F), the spherical vesicles are strongly contracted in the equator, resembling a cell division. If the protein curvature C_p is fixed at a small value, e.g., $C_pR_0 = 9$, gradually increasing θ almost does not change the vesicle shape (Fig. 4(c)). However, for large enough C_p, a division shape minimizes the total free energy at smaller θ and a rugby shape becomes the energy minimum at larger θ (Fig. 4(d)).

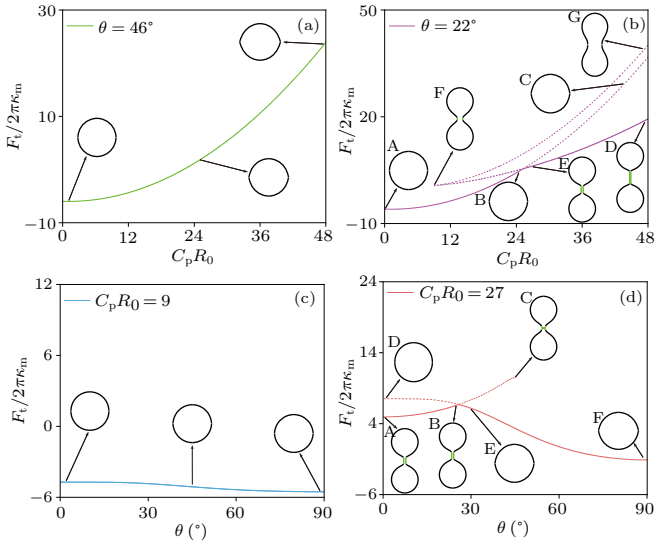


Fig. 4. Free energy curves and the associated shape transformations of a vesicle induced by varying the protein curvature C_p in (a), (b) or the protein orientation θ in (c), (d). The solid lines indicate the minimum free energy state and the dash lines indicate states with higher free energy. The protein ring is located at the equator where $(A_1+A_2)/(2A_0) = 0.5$, and has bending rigidity $\kappa_p/\kappa_m = 2$.

The shape transformation behaviors are summarized in the phase diagram in which the division shapes are separated from the rugby shapes by a boundary curve. Crossing the boundary will induce a first order transition of the vesicle shapes. Compared with the case when the protein ring is near the north pole, the boundary curve is shifted towards larger C_p when the protein ring is located at the equator (compare the boundaries in Figs. 3 and 5).

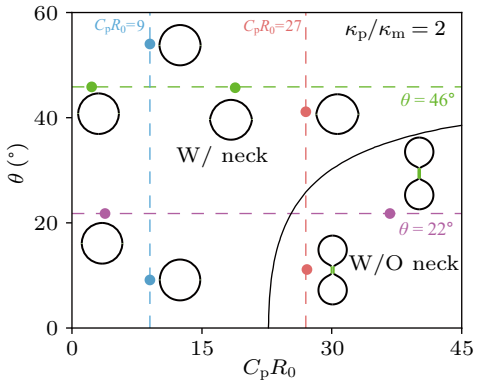


Fig. 5. Phase diagram of vesicle shapes as a function of the protein curvature C_p and the protein orientation θ. The solid line represents the boundary that separates the region of a protrusion shape without a neck from a region with a neck. Crossing the boundary leads to a discontinuous transition of the vesicle morphology. The four colored dashed lines represent the situation studied in Fig. 4. The protein ring is located at the equator where $(A_1+A_2)/(2A_0) = 0.5$, and has bending rigidity $\kappa_p/\kappa_m = 2$.

3.3. Rigid protein coats smooth out the shape transformation

In this section, we fix the position of the protein ring near the north pole and the orientation of proteins at $\theta = 22°$, and show the effects of protein rigidity κ_p on shape transformations of the vesicle. When $\kappa_p/\kappa_m = 2$, as we have shown in Fig. 2(b), with an increasing protein curvature C_p, the free energy curve goes through a Gibbs triangle, which indicates a discontinuous shape transition at the crossing point from a protrusion without a neck to that with a neck (see Fig. 6(a)). With a more rigid protein coat $\kappa_p/\kappa_m = 10$, the size of the Gibbs triangle in the free energy curve is reduced and the transition point is shifted towards smaller curvature values (compare Figs. 6(a) and 6(b)). Upon further increasing the protein rigidity to $\kappa_p/\kappa_m = 79$, the Gibbs triangle disappears and the shape transformation becomes continuous (see Fig. 6(c)). The transition point is further shifted towards a smaller protein curvature C_p.

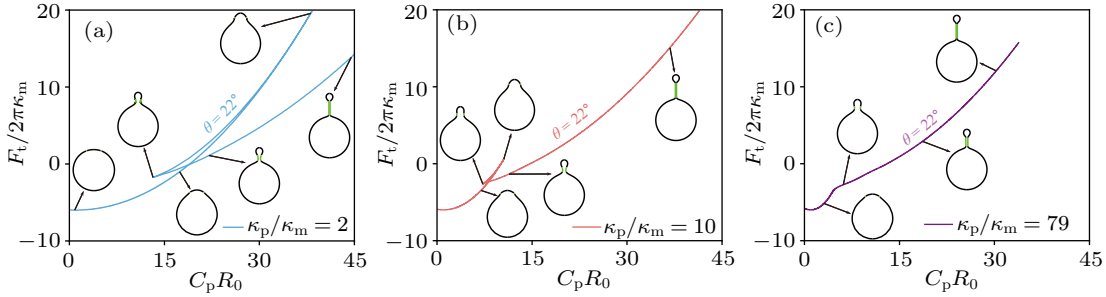


Fig. 6. Free energy curves and the associated shape transformations of a vesicle induced by varying the protein curvature C_p for different protein rigidity. From (a) to (c), the protein rigidity $\kappa_p/\kappa_m = 2, 10, 79$, respectively. The protein ring is located near the north pole where $(A_1+A_2)/(2A_0) = 0.033$. The protein orientation is fixed at $\theta = 22°$.

3.4. Rotating the protein orientation significantly reduces the neck radius

We have shown that upon increasing the protein curvature C_p, a smaller vesicle can grow out from a larger vesicle and the neck that connects the two vesicles grows narrower and longer at the same time (see the green part on the vesicle in Fig. 2(b)). We have also shown that varying the protein orientation θ is able to reduce the neck radius (Fig. 2(d), from A to B to C). In Fig. 7(a), we plot the neck radius as a function of the tilted angle θ (Fig. 7(a), blue curve). A sharp drop of the neck radius is observed when θ approaches about 45°. Compared with the long tube-shaped neck formed by increasing C_p, the neck formed by varying the protein orientation θ is much shorter and exhibits an hourglass shape, which is similar to previous work on BAR proteins.[59] More strikingly, the neck radius is reduced to a value that is smaller than the reciprocal of the protein's preferred curvature (indicated by the blue and red dots on the y-axis in Fig. 7). Similar necking morphology difference is also observed when the vesicle exhibits a division-like shape by a protein ring located at the equator (Fig. 7(a), red curve). Compared with protein orientation-induced necking, the constriction of the neck radius induced by protein curvature is gentler and the neck shows a tubular shape that stays above the reciprocal of the protein curvature (Fig. 7(b)).

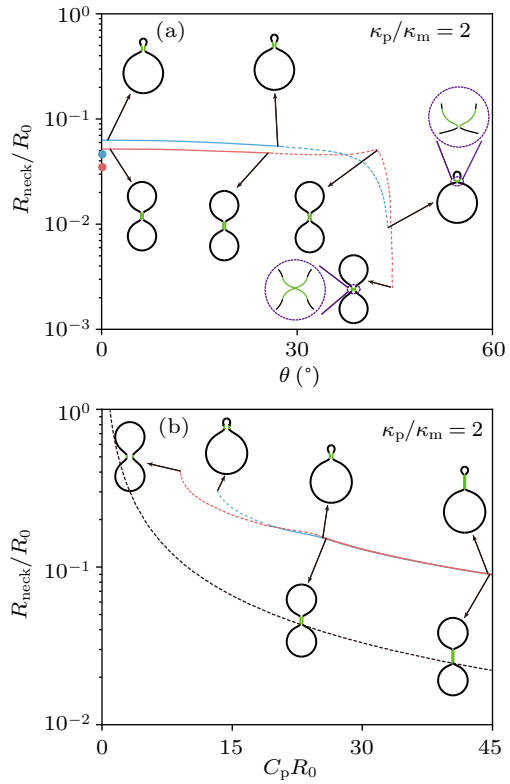


Fig. 7. Contraction of the neck radius induced by varying the protein orientation in (a) and the protein curvature in (b). The blue curve represents the situation that the protein ring is located near the north pole where $(A_1+A_2)/(2A_0) = 0.033$. The red curve represents the case that the protein ring is located at the equator where $(A_1+A_2)/(2A_0) = 0.5$. The solid part indicates the free energy minimum state. The dotted part indicates metastable states which are locally stable but globally unstable. The blue dot and the red dot on the y-axis in (a) indicate the position of the reciprocal of the protein curvature $1/(C_pR_0)$ used to calculate the blue curve and the red curve, respectively. The black dotted curve represents the reciprocal of the protein curvature $1/(C_pR_0)$.

Note that when the tilted angle θ is close to 45°, the necking solution has higher free energy than the one without a neck (plotted in dashed line in Fig. 7). The discontinuous shape transformation occurs at a smaller angle than 45°. However, this does not exclude the physical existence of the necking solution.

In fact, the necking solution represents a metastable state. If θ starts from a smaller value of θ and is gradually increased to 45°, the vesicle shape can remain on the necking branch, and the transition to the other branch needs to overcome a large energy barrier, known as the hysteresis effect.

4. Discussion

In this paper, we study how the orientation of crescent-shaped proteins influences the shape of a vesicle when the proteins are organized into a narrow ring on the vesicle. The underlying assumption behind our model is that proteins can either self-organize into a ring-like structure on the membrane or bind to the membrane by upstream proteins that preassemble into a ring-like structure. Previous studies have shown that BAR proteins can self-organize into a string-like aggregate on the membrane.[41,42] Under certain conditions, the linear aggregate is assembled at the equator and deforms the vesicle into an oblate shape,[41] similar to the shape F shown in Fig. 4(d). A previous study that combines theory with experiments has shown that BAR proteins are spontaneously enriched in the neck region of a membrane template and induce neck elongation, consistent with the shape F shown in Fig. 2. However, as our study is limited to axisymmetric condition, the polygon-shaped vesicle due to several aggregates formed on the vesicle cannot be observed in our work.[41] Extending our continuum theory to more general geometry will be our future endeavor.

Our model also assumes that proteins within the ring are all oriented in the same direction. This is plausible due to the excluded volume effect between the rod-shaped molecules when the protein density is high enough,[43] similar to the entropy-driven isotropic to nematic phase transition for liquid crystals.[60] We neglect the energy contribution associated with the distribution of the protein orientation and set the tilted angle θ as a constant during the vesicle deformation induced by the protein curvature. However, the tilted angle θ might change when the ring is deformed. In a more complete description, the energy contribution associated with the protein orientation should be taken into account and the tilted angle θ should be a function of the free energy and the value of θ over space should be obtained by minimizing the free energy

with respect to θ. In addition to the entropic interaction mentioned above, we expect the chirality of the proteins would also induce a tilted angle, such as the helical band formed by dynamins. Investigating how the chirality of proteins determines the protein orientation would be another future direction to explore.

Necking phenomena are common in cellular processes such as endocytosis and cell division. A vesicle is budding off from the plasma membrane when endocytosis occurs.[16] In mammalian cells, the budding is generally attributed to the dynamin protein that is observed to form a helical band around the neck.[61,62] The chemical energy released by GTP hydrolysis is used to power the constriction of the dynamin. In yeast cells, the role of BAR proteins in driving membrane fission remains controversial.[23,63] It is reported that the switch of the nematic order of anisotropic proteins can contribute to the division shape.[52] There are studies suggesting BAR proteins can actively constrict the neck of the endocytic pit, therefore driving membrane fission.[64,65] It is also reported that BAR proteins recruit dynamin to the neck of the membrane buds to facilitate membrane scission.[66] Our study provides a new angle from the protein orientation to explain the constriction of membrane neck by dynamin or BAR proteins. The fact that they are organized into a helical string, in which the proteins are tilted relative to the azimuthal direction, has a physical reason behind it. The preferred radii of BAR family proteins are typically greater than 10nm. However, in order to pinch off the membrane neck, the neck radius needs to be reduced to ~ 5 nm, the same as the thickness of lipid bilayer. Our results suggest that only in a tilted organization can the protein ring constrict the membrane neck to a value that is smaller than the protein curvature. Therefore, the constriction function of dynamin or BAR proteins powered by GTP hydrolysis is probably due to reorganization of the helical structure into a more tilted manner.

5. Conclusion

In this work, we study the deformation of an axisymmetric vesicle induced by crescent-shaped proteins that assemble into a ring on the vesicle and are oriented in the same direction within the ring. We have shown that when the protein coat is relatively rigid, varying the protein curvature or the protein orientation induces a discontinuous shape transformation of the vesicle from a protrusion without a neck to that with a neck. A very rigid protein coat can smooth out the transition and move the transition point towards a smaller protein curvature. Furthermore, we show that varying the protein orientation alone is able to induce an hourglass-shaped narrow neck. Our study provides a rationale of the helical band formed by BAR proteins or dynamin proteins when they carry out membrane fission functions during endocytosis. Our study also reveals the importance of the organization of the protein aggregates in reshaping the membrane, which is typically neglected in previous researches.

Appendix A: Lagrangian multipliers to enforce geometric relations

The geometric relations expressed by Eqs. (2), (3) and (6) are imposed by introducing three Lagrangian multiplier functions $\alpha(u)$, $\beta(u)$ and $\gamma(u)$ in the functional,

$$F_{\mathrm{L}} = \int_0^1 f_{\mathrm{L}}\,\mathrm{d}u, \tag{A1}$$

in which

$$\begin{aligned} f_{\mathrm{L}} = {} & \alpha(u)\left(\frac{\mathrm{d}r}{\mathrm{d}u} - h\cos\psi\right) + \beta(u)\left(\frac{\mathrm{d}z}{\mathrm{d}u} + h\cos\psi\right) \\ & - \gamma(u)\left(\frac{\mathrm{d}\bar{A}}{\mathrm{d}u} - rh\right). \end{aligned} \tag{A2}$$

Here $\bar{A} = A/(2\pi)$ is the reduced surface area function. With these Lagrangian multipliers, the geometric variables $r(u)$, $z(u)$, $\psi(u)$, $h(u)$ and $A(u)$ become independent. Note that $\gamma(u)$ serves as the membrane tension. If the membrane is inhomogeneous with $A(u)$-dependent membrane properties, variation against $A(u)$ leads to an equation about $\mathrm{d}\gamma/\mathrm{d}u$ in Eq. (B6). The same equation is also derived in Ref. [67].

Appendix B: Variational equations of the composed system

Combining the free energy of the membrane in Eq. (7) and of the proteins in Eq. (9), as well as the Lagrangian multipliers (A1), we arrive at the effective total free energy

$$F_{\mathrm{tot}} = 2\pi\int_0^1 \mathcal{F}[r,z,h,\psi,\bar{A},\alpha,\beta,\gamma]\,\mathrm{d}u, \tag{B1}$$

in which

$$\begin{aligned} \mathcal{F} = {} & \frac{\kappa_{\mathrm{m}}}{2}\left(\frac{1}{h}\frac{\mathrm{d}\psi}{\mathrm{d}u} + \frac{\sin\psi}{r} - C_{\mathrm{m}}\right)^2 rh \\ & + \frac{\kappa_{\mathrm{c}}[\bar{A}(u)]}{2}\left(\frac{\sin\psi}{r}\cos^2\theta + \frac{1}{h}\frac{\mathrm{d}\psi}{\mathrm{d}u}\sin^2\theta - C_{\mathrm{p}}\right)^2 rh \\ & + \frac{p}{2}r^2 h\sin\psi + \alpha(u)\left(\frac{\mathrm{d}r}{\mathrm{d}u} - h\cos\psi\right) \\ & + \beta(u)\left(\frac{\mathrm{d}z}{\mathrm{d}u} + h\cos\psi\right) - \gamma(u)\left(\frac{\mathrm{d}\bar{A}}{\mathrm{d}u} - rh\right). \end{aligned} \tag{B2}$$

The list of Euler–Lagrange equations derived from variations with respect to the functions in Eq. (13) reads

$$\begin{aligned} \psi'' = {} & \frac{h}{2r^2\left(\kappa_{\mathrm{m}} + \kappa_{\mathrm{c}}\sin^4\theta\right)}\left\{h\left[\sin 2\psi\left(\kappa_{\mathrm{m}} + \kappa_{\mathrm{c}}\cos^4\theta\right)\right]\right. \\ & + 2r\left[\alpha\sin\psi + \cos\psi\left(\beta - C_{\mathrm{p}}\kappa_{\mathrm{c}}\cos 2\theta\right)\right] \\ & \left. - 2\frac{\mathrm{d}\kappa_{\mathrm{c}}}{\mathrm{d}\bar{A}}r^2\sin^2\theta\cos^2\theta\sin\psi\right. \end{aligned}$$

$$+r^3\left(p\cos\psi+2\frac{\mathrm{d}\kappa_\mathrm{c}}{\mathrm{d}\bar{A}}C_\mathrm{p}\sin^2\theta\right)$$
$$-2r\psi'\left(\kappa_\mathrm{m}\cos\psi+\kappa_\mathrm{c}\sin^4\theta\cos\psi+r^2\sin^4\theta\frac{\mathrm{d}\kappa_\mathrm{c}}{\mathrm{d}\bar{A}}\right)\Big\}, \tag{B3}$$

$$\alpha'=\frac{1}{2}C_\mathrm{m}^2\kappa_\mathrm{m}h+phr\sin\psi-\frac{\kappa_\mathrm{m}h\sin^2\psi}{2r^2}+h\gamma$$
$$+\frac{1}{2}C_\mathrm{p}^2h\kappa_\mathrm{c}-\frac{\kappa_\mathrm{c}h\sin^2\psi\cos^4\theta}{2r^2}-C_\mathrm{m}\kappa_\mathrm{m}\psi'$$
$$-C_\mathrm{p}\kappa_\mathrm{c}\psi'\sin^2\theta+\frac{(\psi')^2}{2h}\left(\kappa_\mathrm{m}+\kappa_\mathrm{c}\sin^4\theta\right), \tag{B4}$$

$$\beta'=0, \tag{B5}$$

$$\gamma'=-\frac{\mathrm{d}\kappa_\mathrm{c}}{\mathrm{d}\bar{A}}\frac{\left[h\left(C_\mathrm{p}r-\cos^2\theta\sin\psi\right)-r\psi'\sin^2\theta\right]^2}{2rh}. \tag{B6}$$

Note that the variation with respect to $h(u)$ does not give an independent equation but a conserved quantity

$$\mathcal{H}=-\frac{h}{2r}\left\{pr^3\sin\psi+r^2\left(C_\mathrm{m}^2\kappa_\mathrm{m}+2\gamma+C_\mathrm{p}^2\kappa_\mathrm{c}\right)\right.$$
$$+\sin^2\psi\left(\kappa_\mathrm{m}+\kappa_\mathrm{c}\cos^4\theta\right)$$
$$\left.-2r\left[\alpha\cos\psi+\sin\psi\left(C_\mathrm{m}\kappa_\mathrm{m}-\beta+C_\mathrm{p}\kappa_\mathrm{c}\cos^2\theta\right)\right]\right\}$$
$$+\frac{r(\psi')^2}{2h}\left(\kappa_\mathrm{m}+\kappa_\mathrm{c}\sin^4\theta\right). \tag{B7}$$

Meanwhile, we set boundary conditions as

$$\begin{aligned}&\psi(u=0)=0,\quad r(u=0)=0,\\&\beta(u=0)=0,\quad \mathcal{H}(u=0)=0,\\&\bar{A}(u=0)=0,\quad \psi(u=1)=\pi,\\&r(u=1)=0,\quad z(u=1)=0,\\&\bar{A}(u=1)=\bar{A}_0.\end{aligned} \tag{B8}$$

Equations (B3)–(B6) and the geometric relations (2), (3), (6) constitute the full set of equations we need to solve. They together make up 8 first order ordinary differential equations that define a boundary value problem with the unknown constant h, and the 9 boundary conditions given in Eq. (B8).

Appendix C: Numerical methods to solve the variational equations

We solve the boundary value problem with the MATLAB solver bvp5c in an iterative manner. For instance, in order to calculate the shape transformations induced by varying the protein curvature C_p, we start with $C_\mathrm{p}=0$ where the membrane is almost a sphere. Once we get the solution at $C_\mathrm{p}=0$, we can extend the solution to higher values of C_p with a number of small increment of ΔC_p and use the solution of the previous step as a guess for the current step.

When there are multiple branches of solutions, continuously varying C_p could lead to error report due to no solutions beyond certain value of C_p (see the branch from A to B to C in Fig. 2(b)). We then change the iterative variable from C_p to $D_\mathrm{H}=z(0)-z(1)$ which is the pole-to-pole distance by adding a new boundary condition in Eq. (B8). Accordingly, we set the protein curvature C_p as an unknown parameter. By alternating the iterative variables between C_p and D_H, we can obtain the complicated free energy curve with Gibbs triangle. Our MATLAB code is available at the link https://github.com/ruima86/Protein-Orientation.

Acknowledgements

We acknowledge financial support from the the National Natural Science Foundation of China (Grant Nos. 12474199 (RM) and 12374213 (YC)), Fundamental Research Funds for Central Universities of China (Grant No. 20720240144 (RM)), and 111 Project (Grant No. B16029).

References

[1] Decamilli P, Takei K and Mcpherson P 1995 *Current Opinion in Neurobiology* **5** 559
[2] Schmid S, McNiven M and De Camilli P 1998 *Current Opinion in Cell Biology* **10** 504
[3] Turlier H, Audoly B, Prost J and Joanny J F 2014 *Biophysical Journal* **106** 114
[4] Maitre J L, Turlier H, Illukkumbura R, Eismann B, Niwayama R, Nedelec F and Hiiragi T 2016 *Nature* **536** 344
[5] Patra S, Chowdhury D and Juelicher F 2022 *Physics Reports* **987** 1
[6] Antonny B 2006 *Current Opinion in Cell Biology* **18** 386
[7] Zheng B, Meng Q T, Robin Selinger L B, Selinger J V and Ye F F 2015 *Chin. Phys. B* **24** 68701
[8] Schmid S 1997 *Annual Review of Biochemistry* **66** 511
[9] Lichte B, Veh R, Meyer H and Kilimann M 1992 *EMBO Journal* **11** 2521
[10] Sakamuro D, Elliott K, WechslerReya R and Prendergast G 1996 *Nature Genetics* **14** 69
[11] Shimada A, Niwa H, Tsujita K, Suetsugu S, Nitta K, Hanawa-Suetsugu K, Akasaka R, Nishino Y, Toyama M, Chen L, Liu Z J, Wang B C, Yamamoto M, Terada T, Miyazawa A, Tanaka A, Sugano S, Shirouzu M, Nagayama K, Takenawa T and Yokoyama S 2007 *Cell* **129** 761
[12] Takahashi Y, Meyerkord C L and Wang H G 2009 *Cell Death and Differentiation* **16** 947
[13] Laporte D, Coffman V C, Lee I J and Wu J Q 2011 *Journal of Cell Biology* **192** 1005
[14] Zajac A L, Goldman Y E, Holzbaur E L F and Ostap E M 2013 *Current Biology* **23** 1173
[15] McIntosh B B, Pyrpassopoulos S, Holzbaur E L and Ostap E M 2018 *Current Biology* **28** 236
[16] Boulakirba S, Macia E, Partisani M, Lacas-Gervais S, Brau F, Luton F and Franco M 2014 *Proc. Natl. Acad. Sci. USA* **111** 9473
[17] Itoh T, Erdmann K, Roux A, Habermann B, Werner H and De Camilli P 2005 *Developmental Cell* **9** 791
[18] Yang C, Hoelzle M, Disanza A, Scita G and Svitkina T 2009 *PLoS One* **4** e5678
[19] Hartig S M, Ishikura S, Hicklen R S, Feng Y, Blanchard E G, Voelker K A, Pichot C S, Grange R W, Raphael R M, Klip A and Corey S J 2009 *Journal of Cell Science* **122** 2283
[20] Itoh T, Erdmann K S, Roux A, Habermann B, Werner H and De Camilli P 2005 *Developmental Cell* **9** 791
[21] Neumann S and Schmid S L 2013 *Journal of Biological Chemistry* **288** 25119
[22] Qualmann B, Koch D and Kessels M M 2011 *EMBO Journal* **30** 3501
[23] Farsad K, Ringstad N, Takei K, Floyd S, Rose K and De Camilli P 2001 *Journal of Cell Biology* **155** 193
[24] Gallop J L, Jao C C, Kent H M, Butler P J G, Evans P R, Langen R and T McMahon H 2006 *EMBO Journal* **25** 2898

[25] Mim C, Cui H, Gawronski-Salerno J A, Frost A, Lyman E, Voth G A and Unger V M 2012 *Cell* **149** 137

[26] Li Z L 2018 *Chin. Phys. B* **27** 38703

[27] Frost A, Perera R, Roux A, Spasov K, Destaing O, Egelman E H, De Camilli P and Unger V M 2008 *Cell* **132** 807

[28] Henne W M, Kent H M, Ford M G J, Hegde B G, Daumke O, Butler P J G, Mittal R, Langen R, Evans P R and McMahon H T 2007 *Structure* **15** 839

[29] Saarikangas J, Zhao H, Pykalainen A, Laurinmaki P, Mattila P K, Kinnunen P K J, Butcher S J and Lappalainen P 2009 *Current Biology* **19** 95

[30] Prevost C, Zhao H, Manzi J, Lemichez E, Lappalainen P, Callan-Jones A and Bassereau P 2015 *Nat. Commun.* **6** 8529

[31] Kabaso D, Bobrovska N, Gozdz W, Gov N, Kralj-Iglic V, Veranic P and Iglic A 2012 *Journal of Biomechanics* **45** 231

[32] Ramesh P, Baroji Y F, Reihani S N S, Stamou D, Oddershede L B and Bendix P M 2013 *Scientific Reports* **3** 1565

[33] Simunovic M, Evergren E, Callan-Jones A and Bassereau P 2019 *Annual Review of Cell and Developmental Biology* **35** 111

[34] Zhao H, Pykäläinen A and Lappalainen P 2011 *Current Opinion in Cell Biology* **23** 14

[35] Chen Z, Shi Z and Baumgart T 2015 *Biophysical Journal* **109** 298

[36] Hatzakis N S, Bhatia V K, Larsen J, Madsen K L, Bolinger P Y, Kunding A H, Castillo J, Gether U, Hedegard P and Stamou D 2009 *Nature Chemical Biology* **5** 835

[37] Mesarec L, Góoźdź W, Iglič V K, Kralj S and Iglič A 2016 *Colloids and Surfaces B: Biointerfaces* **141** 132

[38] Noguchi H 2014 *Europhys. Lett.* **108** 48001

[39] Bobrovska N, Gozdz W, Kralj-Iglic V and Iglic A 2013 *Plos One* **8** e73941

[40] Chan C, Wen H, Lu L and Fan J 2016 *Chin. Phys. B* **25** 18707

[41] Noguchi H 2015 *The Journal of Chemical Physics* **143** 243109

[42] Simunovic M, Srivastava A and Voth G A 2013 *Proc. Natl. Acad. Sci. USA* **110** 20396

[43] Noguchi H, Tozzi C and Arroyo M 2022 *Soft Matter* **18** 3384

[44] Le Roux A L, Tozzi C, Walani N, Quiroga X, Zalvidea D, Trepat X, Staykova M, Arroyo M and Roca-Cusachs P 2021 *Nat. Commun.* **12** 6550

[45] Helfrich W 1973 *Zeitschrift für Naturforschung C* **28** 693

[46] Zhong-can O Y and Helfrich W 1989 *Phys. Rev. A* **39** 5280

[47] Zhan-Chun T 2013 *Chin. Phys. B* **22** 28701

[48] Zhang Y H, McDargh Z and Tu Z C 2018 *Chin. Phys. B* **27** 38704

[49] Kreyszig E 1991 *Differential Geometry* (New York: Dover)

[50] Zhong Q, Wu C X and Ma R 2023 *Chin. Phys. B* **32** 88704

[51] Perutkova S, Kralj-Iglic V, Frank M and Iglic A 2010 *Journal of Biomechanics* **43** 1612

[52] Mesarec L, Gozdz W, Kralj-Iglic V, Kralj S and Iglic A 2023 *Scientific Reports* **13** 10663

[53] Simunovic M, Evergren E, Golushko I, Prevost C, Renard H F, Johannes L, McMahon H T, Lorman V, Voth G A and Bassereau P 2016 *Proc. Natl. Acad. Sci. USA* **113** 11226

[54] Kralj-Iglic V, Pocsfalvi G, Mesarec L, Sustar V, Hagerstrand H and Iglic A 2020 *PLoS One* **15** e0244796

[55] Mesarec L, Drab M, Penič S, Kralj-Iglič V and Iglič A 2021 *International Journal of Molecular Sciences* **22** 2348

[56] Kabaso D, Bobrovska N, Góźdź W, Gongadze E, Kralj-Iglič V, Zorec R and Iglič A 2012 *Bioelectrochemistry* **87** 204

[57] Kralj-Iglic V, Heinrich V, Svetina S and Zeks B 1999 *Euro. Phys. J. B* **10** 5

[58] Kralj-Iglic V, Babnik B, Gauger D R, May S and Iglic A 2006 *J. Stat. Phys.* **125** 727

[59] Xiao K, Wu C X and Ma R 2023 *Phys. Rev. Res.* **5** 023176

[60] Onsager L 1949 *Annals of the New York Academy of Sciences* **51** 627

[61] Hinshaw J 2000 *Annual Review of Cell and Developmental Biology* **16** 483

[62] Sweitzer S and Hinshaw J 1998 *Cell* **93** 1021

[63] Meinecke M, Boucrot E, Camdere G, Hon W C, Mittal R and McMahon H T 2013 *Journal of Biological Chemistry* **288** 6651

[64] Kukulski W, Schorb M, Kaksonen M and Briggs J A G 2012 *Cell* **150** 508

[65] Kishimoto T, Sun Y, Buser C, Liu J, Michelot A and Drubin D G 2011 *Proc. Natl. Acad. Sci. USA* **108** E979

[66] Hohendahl A, Talledge N, Galli V, Shen P S, Humbert F, De Camilli P, Frost A and Roux A 2017 *eLife* **6** e26856

[67] Agrawal A and Steigmann D J 2009 *Biomechanics and Modeling in Mechanobiology* **8** 371